Applied Energy 86 (2009) 96–105

Contents lists available at ScienceDirect

Applied Energy

journal homepage: www.elsevier.com/locate/apenergy

Variable valve timing for fuel economy improvement in a small spark-ignition engine

G. Fontana, E. Galloni *

Department of Industrial Engineering – University of Cassino, Via G. De Biasio 43, Cassino, Italy

ARTICLE INFO

Article history:
Received 12 February 2008
Received in revised form 9 April 2008
Accepted 11 April 2008
Available online 6 June 2008

Keywords:
SI engine
VVT
Internal EGR
Reverse Miller cycle
Variable swirl
CFD analyzes

ABSTRACT

The potential of a simple variable valve timing (VVT) system has been investigated. This system has been designed to update a small displacement engine pursuing the objective of optimizing both engine performance and, particularly, fuel consumption at part load operation. A continuously variable cam phaser (CVCP), able to produce a reverse Miller cycle effect during the intake phase and a significant internal EGR generation at the end of the exhaust stroke, has been introduced. A numerical approach, based on both 1-D and 3-D computational models, has been adopted in order to evaluate the engine performance when load is controlled by the VVT system and to deeply investigate the influence, on in-cylinder phenomena, of the valve timing variation. In this way, the VVT system here analyzed revealed as an effective tool in reducing the pumping losses, hence the specific fuel consumption, at partial load.

© 2008 Elsevier Ltd. All rights reserved.

1. Introduction

The European Union has recently signed the Kyoto protocol. Thus, the control of green-house gas emissions has begun to add to the numerous constraints that vehicle manufacturers have to satisfy. The reduction of engine fuel consumption becomes a primary requirement as well as meeting current and future emission legislations.

Naturally, talking about reduction of engine fuel consumption means to keep unvaried, sometimes improved, the performance level of current engine production. Dealing with engine topics exclusively, improving fuel economy to reduce CO_2 emissions means improving the engine thermal efficiency.

As it is usual in engine management, this target can be met following different routes, each of them could be an effective way with different cost-to-benefit ratio. Often, it could be observed, it is helpful to adopt numerous solutions contemporaneously. As an example, fast combustion, lean burn, variable valve timing and actuation, gasoline direct injection and so long may be reminded.

During most of its average life, a road engine is run under low load and low speed conditions. It is known that load reduction in spark-ignition engines is traditionally realized by introducing additional losses during the intake stroke by means of a throttle valve. In these operating points, the engine efficiency decreases from the peak values (already not very high) to values dramatically lower.

The optimization of intake and exhaust valve timing can provide significant reductions in pumping losses at part load operation [1–3]. In this paper, the benefit of engine load control performed by using a simple variable cam phaser has been analyzed and the influence of the VVT strategy on the combustion process and engine performance has been evaluated.

1.1. The engine

The engine under study (Table 1) derives from a small displacement (1.4 l), 2 valves per cylinder, MPI engine developed in late 1980s.

The objective of this paper is to contribute to the development of an up-to-date version pursuing, among others, the target of improving engine fuel economy. To this aim, the adoption of a continuous variable valve timing (VVT) system, able to optimize engine torque and efficiency, has been considered [4].

In particular, the VVT technology here proposed is mainly aimed to the load control and the generation of internal exhaust gas recycle (EGR) rather than to the volumetric efficiency optimization. Due to economic constraints, the engine architecture with a single camshaft for the valve actuation has been kept.

A continuously variable cam phaser (CVCP), able to shift the overhead camshaft to retarded positions at constant overlap [5] (Fig. 1), has been chosen. This simple and economic system allows a load control shared between CVCP and throttle. Delaying all valve

* Corresponding author. Tel.: +39 776 2994005.
E-mail addresses: fontana@unicas.it (G. Fontana), galloni@unicas.it (E. Galloni).

0306-2619/$ - see front matter © 2008 Elsevier Ltd. All rights reserved.
doi:10.1016/j.apenergy.2008.04.009

Table 1
Main baseline engine characteristics

Total piston displacement (cm^3)	1368
Bore (mm)	72.0
Stroke (mm)	84.0
Cylinder number	4
Valve number	8
Geometrical compression ratio (–)	11.0
Valve timing (Intake–exhaust) (°)	7/41–55/–7

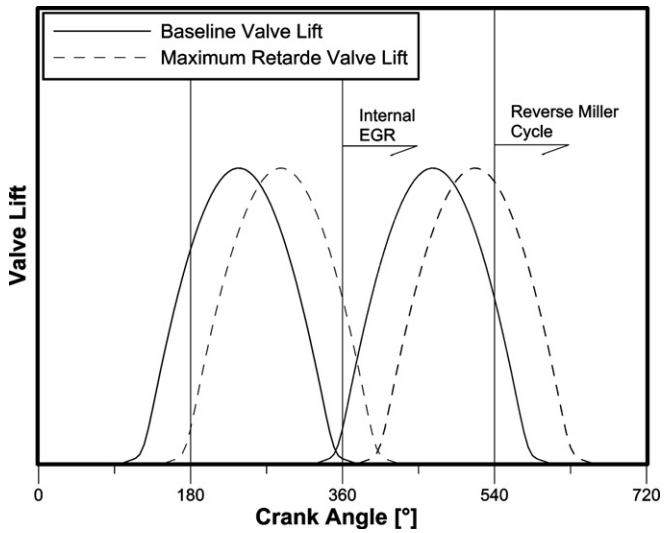

Fig. 1. Due to exhaust gas re-aspiration and intake backflow, retarded valve events penalize the engine volumetric efficiency. At wide open throttle, delaying the valve timing the engine load decreases while the internal EGR ratio increases. (Dashed line: exhaust valve lifts; solid line: intake valve lifts).

events, an intensive backflow at the intake end occurs (reverse miller cycle) and a large amount of exhaust gas comes back into the cylinder (internal EGR).

Combining reverse miller cycle and internal EGR a significantly high de-throttling effect can be achieved, thus reducing the pumping losses at part load and improving the fuel economy in many driving conditions.

Obviously, the engine load control by means of the CVCP system at fully un-throttled operation is limited by the EGR tolerance of the engine. In order to improve this engine characteristic at medium and low loads, when the engine is operated at high EGR rate, a particular exhaust port geometry, able to generate a variable swirl motion of recirculated exhaust gases, has been designed. In detail, an exhaust valve masking has been adopted in order to generate an intensive swirl motion of the re-aspirated exhaust at low valve lifts. Combining this effect with the swirl motion generated during the late intake process allows obtaining a high turbulence level at part load, improving the combustion quality and making tolerable high charge dilutions. (in Fig. 2, some details of the prototype engine are illustrated). Thus, optimized port-valve designs could provide high turbulence levels and high volumetric efficiency in order to achieve both satisfying fuel economy at part load and appreciable full load performance.

2. Numerical approach

CFD modeling has been utilized in order to both understand the engine in-cylinder phenomena and provide guide lines for the experimental tests aimed to find the optimal solutions.

Preliminary analyzes have been carried out to estimate the behaviour of the baseline engine using the CVCP system. A numerical analysis has been performed by means of a 1-D code able to simulate the whole thermodynamic cycle.

These preliminary results showed the effectiveness of this approach. The high calculated EGR rates showed the need of improving the in-cylinder turbulence level in order to obtain optimal combustion rates and stability at medium and low loads. The generation of a swirl motion, produced by the recirculated exhaust gases, has been considered to reach this target.

Furthermore, 3-D analyzes have been carried out in order to obtain both a correct design of the exhaust port (steady-flow analysis) and a sound explanation of the phenomena occurring when the engine valve timing yields deep modifications of the in-cylinder flow field and combustion process (transient analysis).

The 3-D simulations have been performed by the 7.3b standard release of the AVL FIRE code [6,7]. The processor allows solving the ensemble-averaged governing equations of the flow and the heat transfer within the computational domain either for steady-state or for transient analysis in moving grids. For engine applications, the code dynamically modifies the grid according to the valve lift diagram and the piston kinematics; the rezone subroutine allows re-mapping the calculated field between grids with different resolutions. The problem of the unknown turbulence correlation is resolved through a compressible version of the standard two equations k–ε model. The partial differential transport equations are discretized on the basis of a finite volume method. The temporal discretization is Euler implicit. Hybrid and CTVD differencing schemes are used for the approximation of the spatial derivatives. The coupled set of algebraic equations is solved iteratively based on a pressure–velocity coupling procedure. Each algebraic equation system is worked out by the GCCG solver (Orthomin solver) [8].

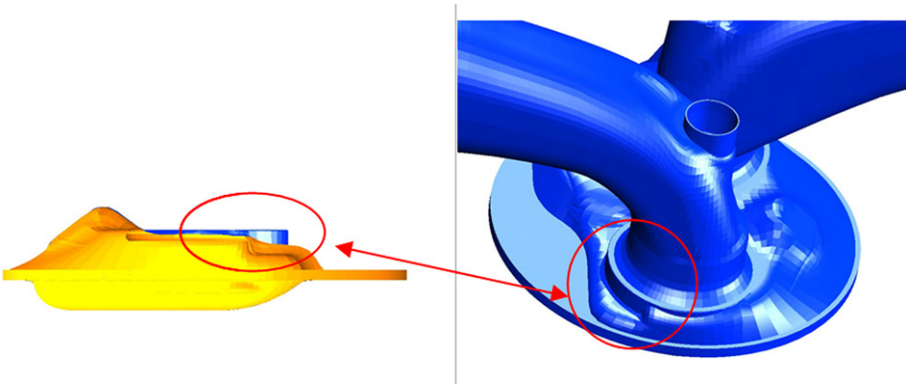

Fig. 2. Combustion chamber cross section (left), ducts and combustion chamber drawing (right). The valve masking is highlighted.

The complex oxidation process of gasoline fuel during the turbulent combustion process is modeled by a single step irreversible reaction Eq. (1), then five chemical species (Fuel, O_2, N_2, CO_2 and H_2O) are considered

$$\text{Fuel} + O_2, \quad N2 \rightarrow \text{products}(CO_2,\ H_2O) + N_2 \tag{1}$$

Three transport equations for the density weighted mean quantities of fuel mass fraction, mixture fraction and residual gas fraction are solved together with five algebraic expressions to determine the other mass fractions as in Spalding [9]. The solution of this set of equations depends on the determination of the mean reaction rate of Eq. (1) [10,11].

Based on the laminar flamelet concept, the CFM model assumes that the mass burning rate per volume unit is proportional to the laminar flame speed (S_l, Eq. (2)). The proportionality factor is represented by the flame surface density (Σ), determined via a balance equation Eq. (3). In this way, the CFM separates the treatment of the chemical problem, reassumed by the overall variable S_l, and the turbulent interactions described by Σ

$$\dot{w} = \rho_u S_L \Sigma \tag{2}$$

$$\frac{\partial \Sigma}{\partial t} + \frac{\partial}{\partial x_i}(U_i \Sigma) = \frac{\partial}{\partial x_i}\left(\frac{\nu_t}{\sigma_\Sigma}\frac{\partial \Sigma}{\partial x_i}\right) + S - D \tag{3}$$

In Eq. (3), S is the production of the flame surface related to the turbulent strain rate while D is the annihilation term due to mutual collisions. The D term is proportional to Σ^2; S term is proportional to the product of the average rate of strain and the flame surface density Σ via an empirical coefficient. According to the ITNFS model [12,13] the average rate of strain is considered proportional to the reciprocal of the turbulent mixing time corrected by a function which accounts for the size of turbulence scales and for viscous and transient effects. The laminar flame thickness is estimated by assuming the Blint number equal to 2 [14]. The laminar flame speed is supposed depending on the fresh gas conditions, the experimental correlations of Metghalchi and Keck are used [15].

3. Results

Both 1-D and 3-D simulations have been carried out in order to well assess the performance improvement coming from the adoption of the VVT technology in the prototype engine.

3.1. Steady flow analysis

In order to improve the mean in-cylinder swirl motion, a particular exhaust port geometry, able to generate a variable swirl motion of recirculated exhaust gases, has been designed. 3-D steady flow calculations have been carried out to investigate about valve performances.

At several valve lifts, steady flow simulations have been performed by using grids like those reported in Fig. 3. As it is shown, the computational domain reproduces the typical conditions of a steady flow bench.

Unstructured grids have been generated using hexahedral elements. The greatest care was used to well reproduce the exact surface geometry and to discretize the valve.

The solid surfaces are modeled as no-slip walls: according to the industrial manufacture, some of them are considered technically smooth and some rough.

In Fig. 4, calculated discharge coefficients and calculated swirl numbers for the intake port and the exhaust port are shown. The calculated results are relative to the ultimate shape adopted for the engine head.

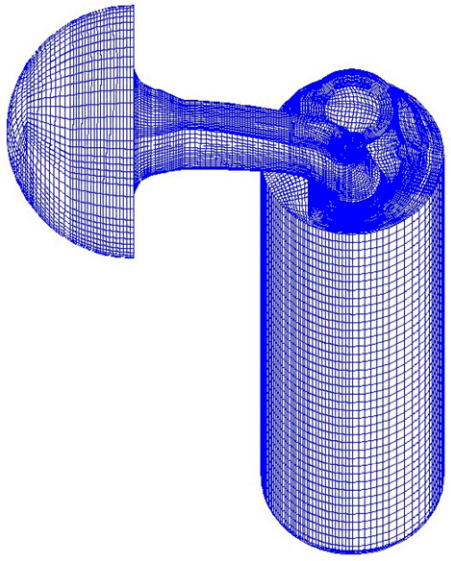

Fig. 3. Computational grids for steady flow tests.

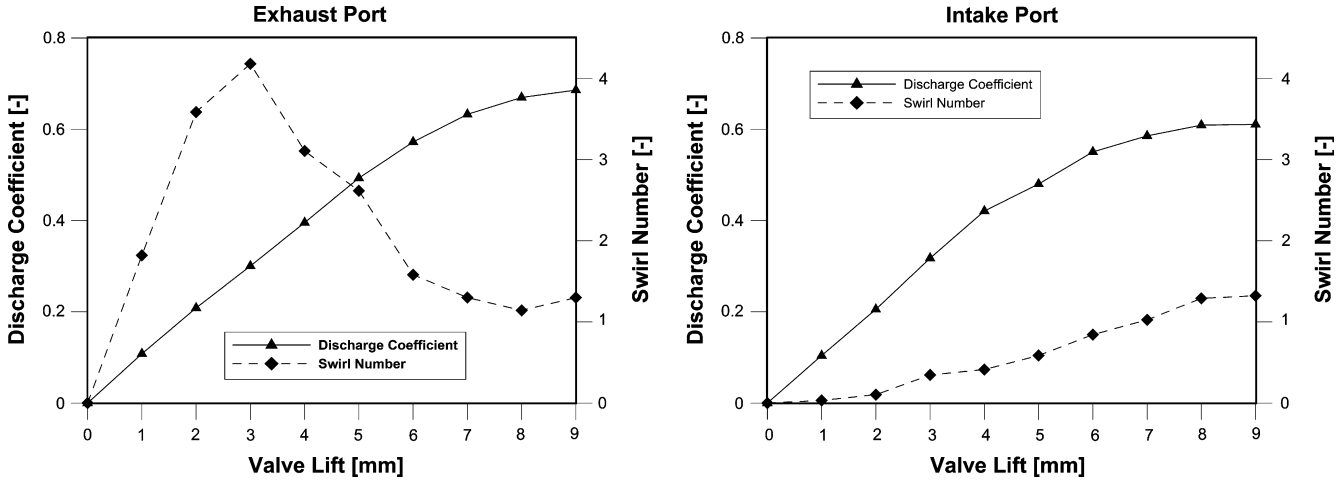

Fig. 4. Calculated discharge coefficients and swirl number for intake and exhaust port. Flow entering the cylinder for both cases.

The discharge coefficient for subsonic compressible flows is calculated considering the isentropic mass flow rate related to the inner seat valve diameter and the pressure ratio across the port as in [16]. The swirl numbers are equivalent to the swirl torque numbers measured in the experimental tests; they are calculated starting from the angular momentum estimated in a plane orthogonal to the cylinder axis, one diameter far from the fire face.

In order to test the potential of the designed geometry in swirl generation during the burned gas reverse flow, the exhaust port has been considered as an intake port.

The conventional tangential port adopted for the intake is able to make a weak swirl at high lifts, while the masked exhaust port allows, at low and middle lifts, to bring the re-aspired gas into the cylinder with a marked tangential direction.

Finally, the calculated discharge coefficients are compared to those measured in experimental tests (Fig. 5). These tests have been performed on an engine prototype made in accordance with the considered geometries. Bearing in mind that, in the experimental tests, an intake valve slightly different with respect to that modeled in CFD calculations has been used (this explains the differences occurring at middle lifts of the intake port), the predicted coefficients are in very good agreement with experimental results. The mean error is of the same magnitude order of that obtained by many other authors [17–19]: this is also a first model verification, before starting to simulate the engine behaviour.

3.2. Performance analysis

The engine performance when load is controlled by valve timing variations has been evaluated by the 1-D modeling.

In order to evaluate the engine performance at different valve timings, a simple combustion model, based on Hires' approach, has been utilized [20]. This thermodynamic model allows describing the combustion development starting from the heat release analysis at a reference operating point.

The model has been validated by comparing the obtained results to those coming from experimental tests carried out at full load conditions on a prototype engine using the port design described in the previous paragraph. At these operating points, the engine has been tested with the standard valve timing (in the following, this valve timing will be called VVT0).

The calculated data have shown a satisfying agreement to the measured data. As an example, measured and calculated volumetric efficiencies are reported in Fig. 6. The maximum error is about 5%, while at low speed, i.e. the operating conditions analyzed in this paper, the deviation is less than 1%.

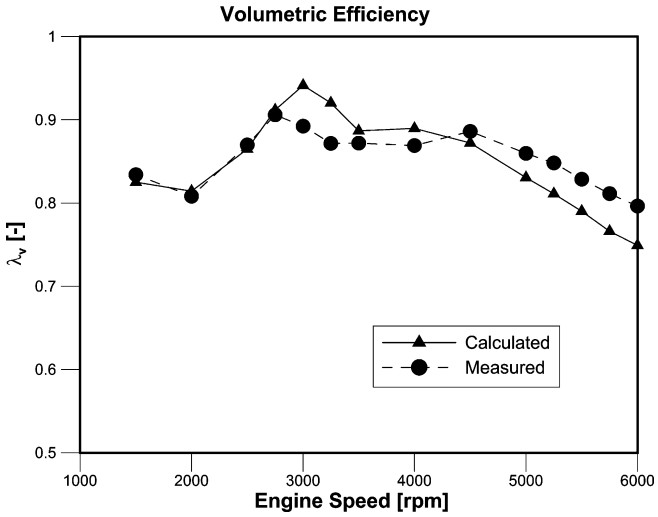

Fig. 6. Comparison of measured and calculated engine volumetric efficiencies at full load.

After validation, the 1-D model has been utilized in order to compare the engine behaviour when load is reduced, from the full load up to a 2 bar mean effective pressure, by means of a traditional throttling (at a given valve timing, VVT0), to that obtainable when load is controlled by both retarded valve times and a lighter throttling.

As it has been illustrated in engine description, the variable cam phaser is able to shift the camshaft to retarded positions at constant overlap. A maximum valve timing delay equal to 54° has been assumed.

At 2000 rpm, the VVT strategy allows reducing load of about 50% without adding the typical throttling losses (Fig. 7). The spark advance is optimized for the maximum brake torque. For further load reductions a combined valve timing-throttle control is necessary. However, the requested throttling degree is lower. Thus, when VVT is used, the pumping mean effective pressure is visibly lower at all load values. In particular, at the minimum analyzed load, the pumping work reduction is 47% (Fig. 8).

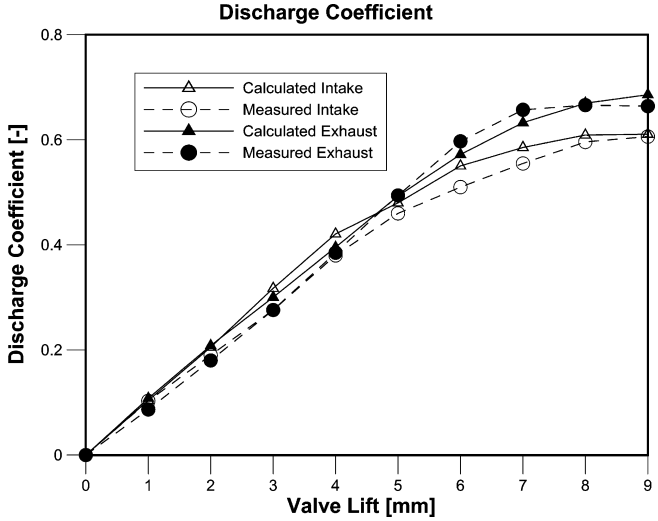

Fig. 5. Comparison of calculated and measured discharge coefficients.

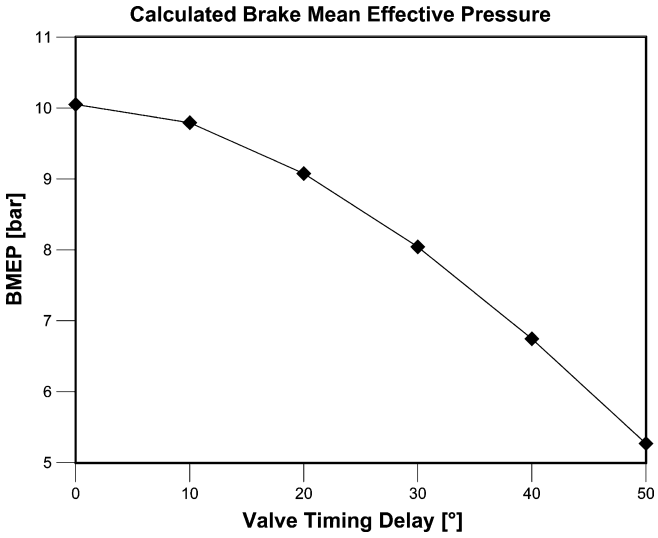

Fig. 7. BMEP values at different cam phaser delayed positions. Speed: 2000 rpm, WOT.

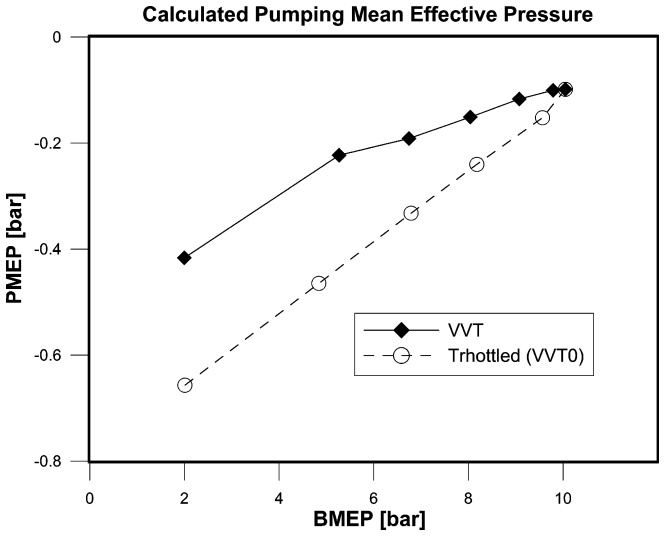

Fig. 8. Mean effective pressure values of the low pressure cycle. Comparison of pure throttle control and combined VVT-throttle control. Speed: 2000 rpm.

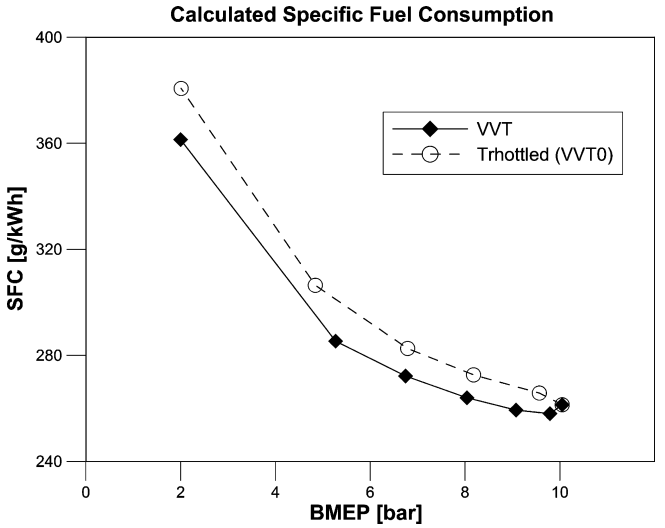

Fig. 10. Comparison of brake specific fuel consumptions calculated for pure throttle load control and throttle-VVT load control.

Naturally, retarded valve close angles induce a considerable reverse flow at the end of both the exhaust and the intake strokes. This yields a volumetric efficiency decrease and an internal exhaust gas recirculation as well.

As a consequence, at 2000 rpm, BMEP = 2 bar, the VVT-throttle control engine shows a calculated EGR ratio equal to 0.23. This value is about 50% higher than that of the baseline engine (Fig. 9).

Finally, Fig. 10 shows a comparison between the specific fuel consumption calculated for pure throttle control and throttle-VVT load control: from full load operation to an IMEP value of 2 bars, the VVT strategy here described allows an improvement in specific fuel consumption of about 5% or 6% with respect to the traditional load control.

3.3. In-cylinder analysis

3-D calculations have been also used to analyze the in-cylinder phenomena occurring at engine part load operation when load is controlled by using both the variable cam phaser and the throttle.

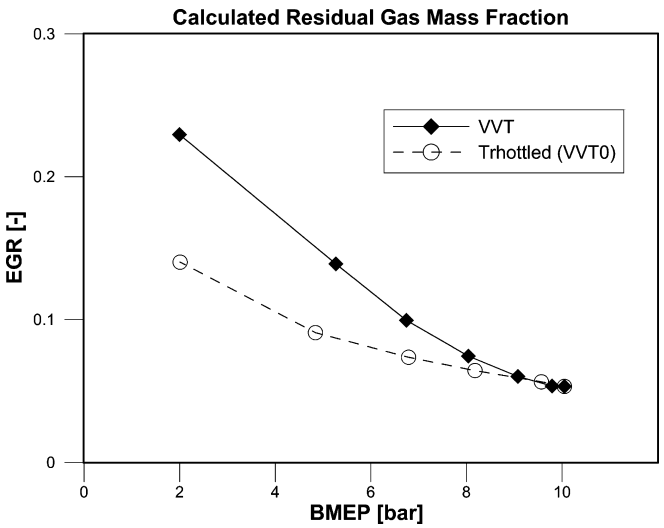

Fig. 9. Calculated residual gas content for pure throttle control and throttle-VVT load control. The EGR ratio is calculated at the intake valve close by dividing the residual mass contained in the cylinder by the total in cylinder–mass.

The operating point characterized by engine speed equal to 2000 rpm, and mean effective pressure equal to 2 bars has been chosen. This point has been obtained considering several cam phaser positions with different throttle opening. The considered valve timing retards (added to the standard engine valve timing) are: 0° (VVT0), 46° (VVT46), 50° (VVT50) and 54° (VVT54).

This approach allows achieving the desired load with a significantly de-throttling effect. For each cam phaser position examined, unstructured dynamic grids have been generated using hexahedral elements according to the procedure described in [21].

As an example, the grid shown in Fig. 11 has got about 170,000 cells as a minimum and about 250,000 cells as a maximum.

For the baseline engine the comparison of calculated and measured in-cylinder pressure is shown in Fig. 12. The characteristic constants used for this model are shown in Table 2.

In order to show the importance of cycle-by-cycle and cylinder-to-cylinder variations, three different measured curves are reported. Considering these variations, the numerical results seem to be satisfactory and they encouraged the authors in using the model to predict the in-cylinder phenomena occurring through the engine cycle.

3.3.1. Gas-exchange analysis

The calculated cylinder pressure vs. cylinder volume during the gas-exchange strokes, relatively to the several valve timings analyzed, is plotted in Fig. 13.

Using late valve timings, pumping work decreases due to the de-throttling effect. Moreover, the delayed exhaust valve close allows increasing the effective expansion ratio and expansion work, without eye-catching consequence for the exhaust pumping work. On the other hand, the higher pressure reached during the suction stroke causes higher compression work.

Nevertheless, the "Miller effect" [22] due to the late intake valve close reduces the effective compression ratio; as a consequence the cylinder pressure increases very weakly when the piston begins to move towards the top dead centre; after the end of the intake phase, the cylinder pressure raises following polytropic curves close to those of the standard valve timing. This limits the increase in compression work.

These favourable effects yield to the actual decrease of the brake specific fuel consumption at part load operation showed in the previous section (Fig. 10).

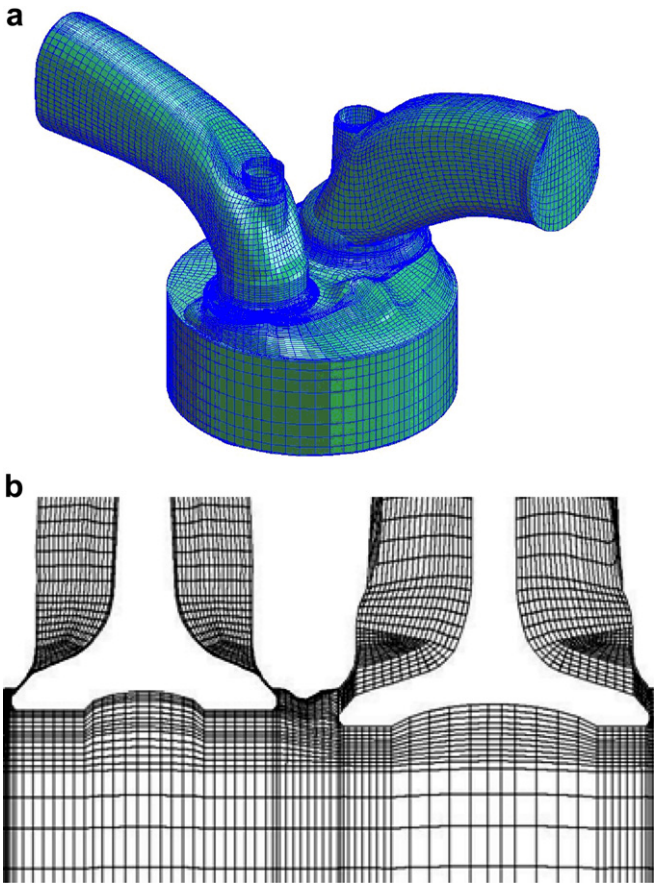

Fig. 11. (a) Engine grid during the valve overlap; cam phaser position VVT50. (b) Valve gap discretization details.

As shown above, extremely retarded angular positions of the cam phaser give rise to large amounts of backflow of fresh charge and burned gas. Large quantities of burned gas can be utilized by the engine both for load control and NO_x reduction provided that combustion quality is not too much reduced.

Fig. 14 shows the calculated EGR field at the intake valve close for the 50 c.a. deg. valve timing delay. It is worth noting that a portion of residual gas flows out of the combustion chamber before the intake valve close.

Table 2
Model characteristic constants

Flame kernel radius [m]	$4 * 10^{-3}$
Initial density [1/m]	300
Production constant	1.1
Destruction constant	1.0

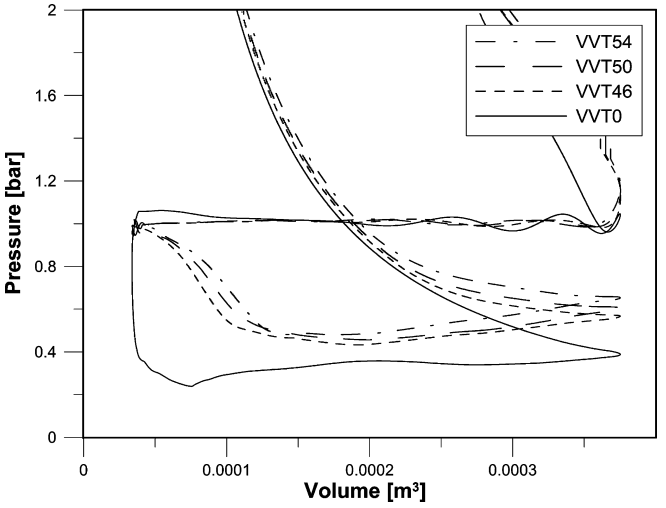

Fig. 13. Pressure–volume diagrams for the considered valve timings. Pressure curves calculated by 3-D computations.

As summarized in Table 3, this matter is negligible for the reference case (VVT0), while a 54 c.a. degrees retard of the valve points leads to a 14.5% of the exhaust gas escaping towards the intake port. Obviously, these burned gases will come back into the cylinder during the next cycle increasing the actual EGR ratio.

Unfortunately, the re-aspirated exhaust gases slow down the engine burning rate, especially at very low loads like those considered in this paper. The high EGR ratio found confirms the necessity to generate opportune turbulence levels in order to allow a stable and fast combustion. So, swirl generation by means of both the exhaust gas backflow and the fresh charge flow entering the cylinder could be very useful in order to accelerate the flame propagation of the diluted charge [23].

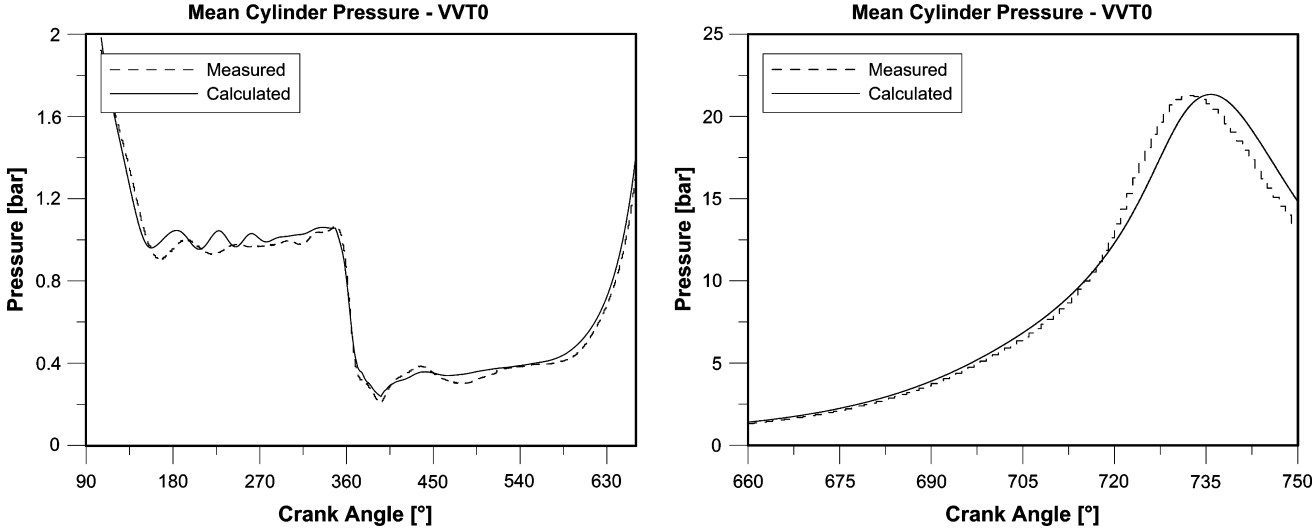

Fig. 12. Comparison of calculated and measured in cylinder pressure curves, 2000 rpm, BMEP = 2 bar, CVCP at 0°. Left: gas-exchange phase; right: high pressure.

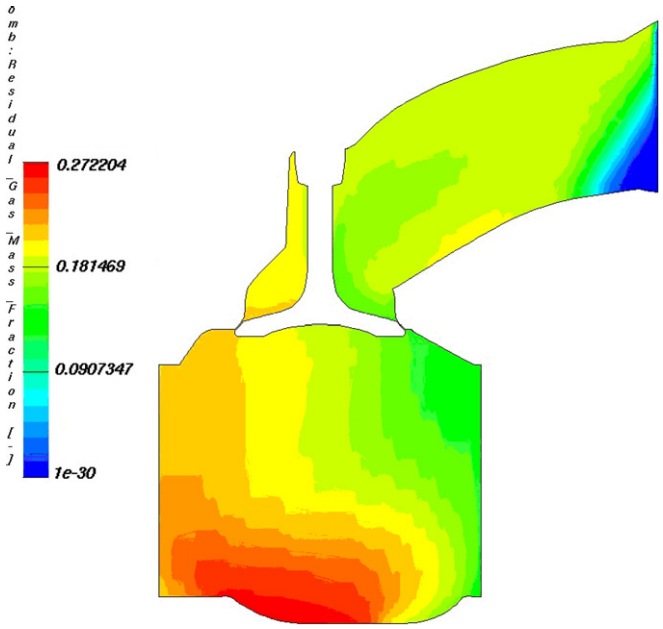

Fig. 14. Residual gas mass fraction at intake valve close, VVT50.

Table 3
Residual gas mass at relevant valve points

VVT [°]	Residual gas mass [kg]	
	Exhaust valve close	Intake valve close
0	1.57E−05	1.55E−05
46	2.45E−05	2.10E−05
50	2.75E−05	2.37E−05
54	2.90E−05	2.51E−05

CFD calculations have been used to analyze the flow pattern produced in this way.

3.3.2. Variable swirl analysis

The swirl number has been defined as follows:

$$SN = \frac{\Gamma}{I \cdot 2 \cdot \pi \cdot rps} \quad (4)$$

where Γ and I are the momentum and the moment of inertia of in-cylinder charge, respectively.

In Fig. 15, the calculated swirl number and the mass flows through the engine ports, for the minimum and maximum valve phase delay, are plotted.

Each swirl curve shows two peaks. As it was already seen, both exhaust and intake ports are able to generate swirl, so the first peak occurs at the maximum reverse flow coming from the exhaust port, while the second one occurs at the maximum flow rate aspirated from the inlet manifold. For the standard valve timing (VVT0), the swirl motion is generated, as usual, during the suction stroke; however, a reverse flow, at the end of the exhaust blow-down phase (150–180 c.a. deg., Fig. 15), produces a weak swirl motion, but it decays during the displacement stroke.

For retarded valve points, the reverse flow entering the cylinder after 360° produces a strong swirl impulse. In fact, a large re-aspirated flow rate crosses the valve at middle and low lifts; in this situation the masked port shows the highest capability in generating the charge rotation. Swirl decreases after exhaust valve close: at low lifts, the intake port is not able to bring the fresh charge into the cylinder with a large momentum while the momentum flow is not enough robust to face the increase of the in-cylinder mass, so the charge rotation slows down. When the intake valve reaches higher lifts, the tangential duct begins to work: the mass flow rate is associated with a large angular momentum flow, so the cylinder swirl increases.

In Fig. 16, a comparison of different swirl numbers obtainable at different cam phaser positions is reported. During compression, highest swirl levels are found for the standard cam phaser position VVT0; the minimum swirl level is found for the VVT50 case. Toward the end of the compression stroke (at 660°, for instance) the maximum calculated swirl number (SN = 1.240) is 14% higher than the minimum (SN = 1.089).

Focusing on the suction stroke, retarding the intake valve open, the maximum mass flow rate, occurring at about half piston stroke, corresponds to middle intake valve lifts; the intake valve reaches the maximum lift (i.e. the best capability in directing the flow) when the piston is close to the bottom dead centre and the aspirated flow rate is very small. As a consequence, a large valve timing delay yields a reduction in swirl generation during the induction stroke; in fact, the maximum intake valve lift is translated towards the bottom dead centre: when the intake port shows the highest capability in generating a swirl motion there is not any flow to direct.

So, it seems a good idea to use the exhaust swirl concept. Retarding the valve points decreases the swirl generation during the induction stroke, but increases the swirl production during the exhaust reverse flow.

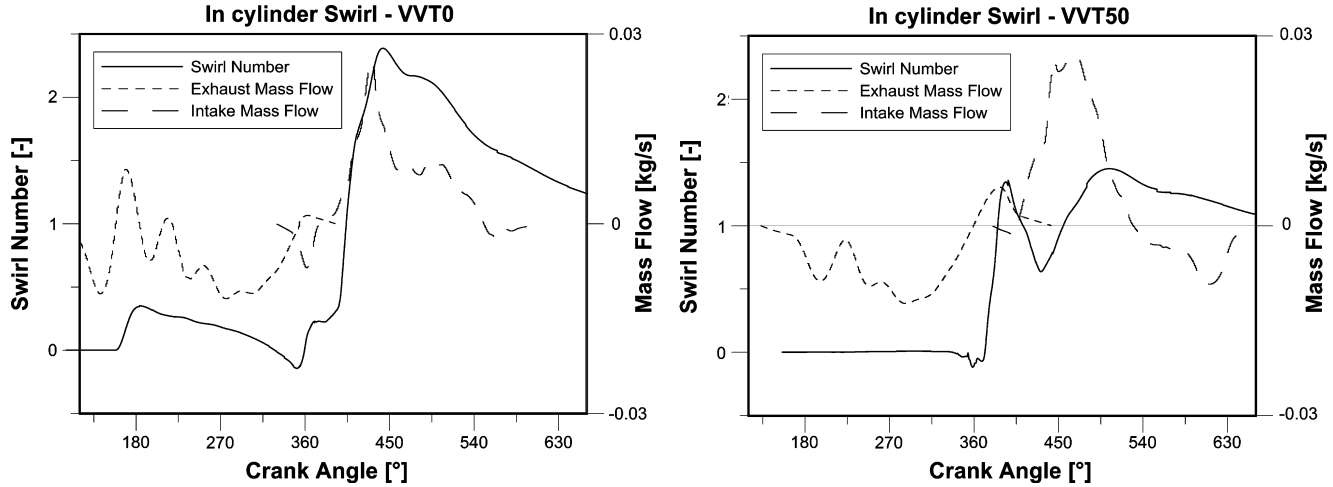

Fig. 15. Calculated in cylinder swirl and mass flow through the ports; for standard (left) and retarded valve timing (right).

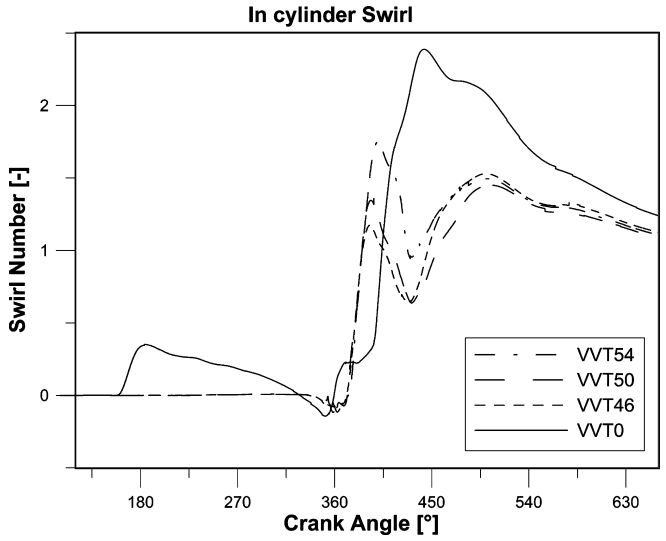

Fig. 16. Comparison of the in-cylinder swirl numbers calculated at different cam phaser positions.

Naturally, the mass flow rate of exhaust gas re-aspirated into the cylinder is much less than the fresh charge entering from the intake; even though the exhaust port performs steady flow swirl indices much higher than those of the intake port, the exhaust stroke weighs, on the whole swirl generation process, much less than the suction stroke.

Fig. 17 shows the benefit provided by the exhaust swirl concept. With respect to the reference case (VVT 0), for which the swirl generation during the exhaust stroke can be neglected, the VVT 50 case shows a meaningful reduction of the in-cylinder swirl, calculated a 660°, when the masked port is not used. Masking the port allows translating the curve of the generated swirl during the intake phase. At 660°, the engine using the exhaust swirl concept shows a swirl level about 13% higher than that obtained by using a traditional port design [24,25].

3.3.3. Combustion analysis

The engine prototype has been tested adopting a delay of 46 and 50 crank angle degrees in the valve timing. Measures have been carried out at 2000 rpm; the throttle opening and the spark-timing have been set to obtain a value of the brake mean effective pressure equal to 2 bar. Less retarded valve events have not been considered in order to obtain high de-throttling effects (i.e. low pumping losses).

The prototype was able to perform a stable combustion phase despite the high EGR rate and the low load. The coefficient of variation of IMEP was less than 3%, backfire or misfire phenomena were not pointed out. Using a valve timing retard of 50 crank angle degrees, the efficiency of the prototype engine has improved of about 5% with respect to the baseline configuration.

Obviously, retarding the CVCP positions, the optimal spark advance significantly increases according to the measured combustion durations (Fig. 18). This effect is a consequence of the large amount of exhaust gas re-aspirated that mainly affects the flame development stage.

The numerical analysis has been done according to the experimental conditions. Fig. 19 shows the capability of the numerical model in predicting the behaviour of the prototype engine operated at retarded valve timings, while in Fig. 20 the calculated high pressure curves, obtained varying the engine valve timings, are reported.

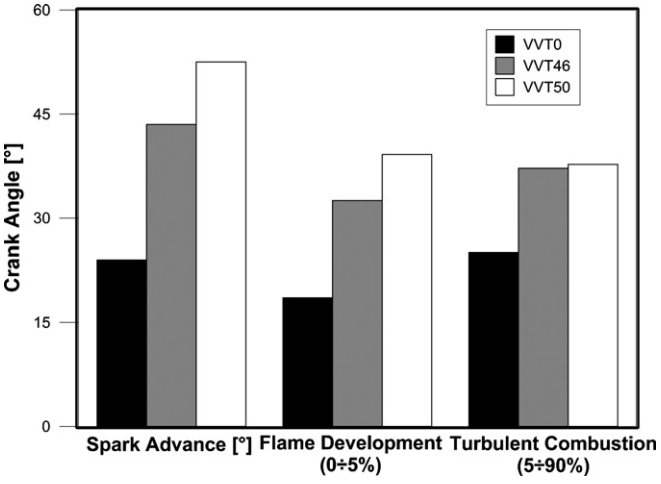

Fig. 18. Spark advance and experimental combustion duration.

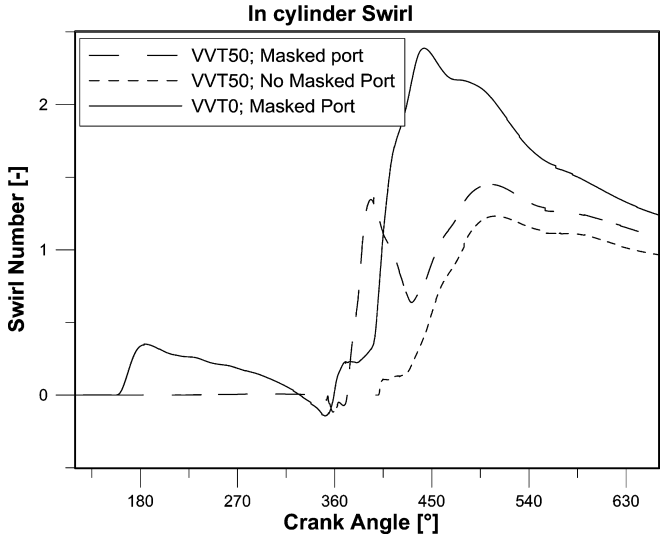

Fig. 17. Comparison of swirl generation with or without exhaust swirl concept.

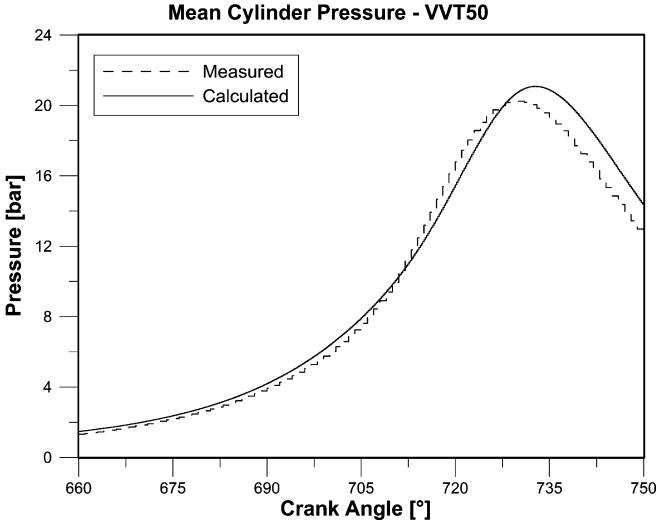

Fig. 19. Comparison of calculated and measured in-cylinder pressure curves, 2000 rpm, BMEP = 2 bar, CVCP at 50°.

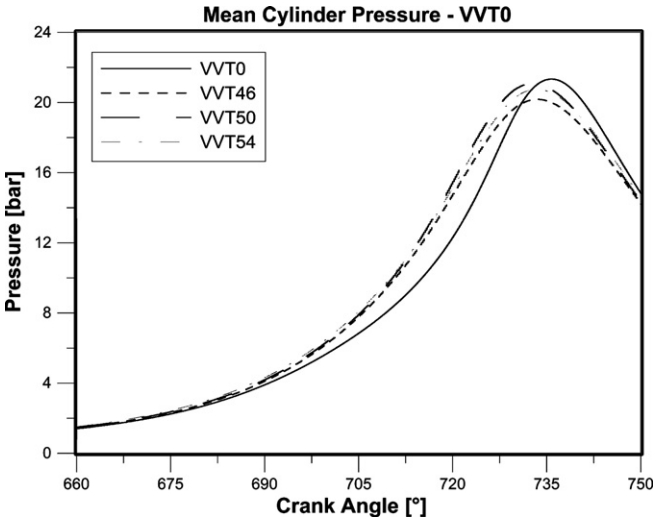

Fig. 20. Comparison of high pressure curves calculated varying the valve timing.

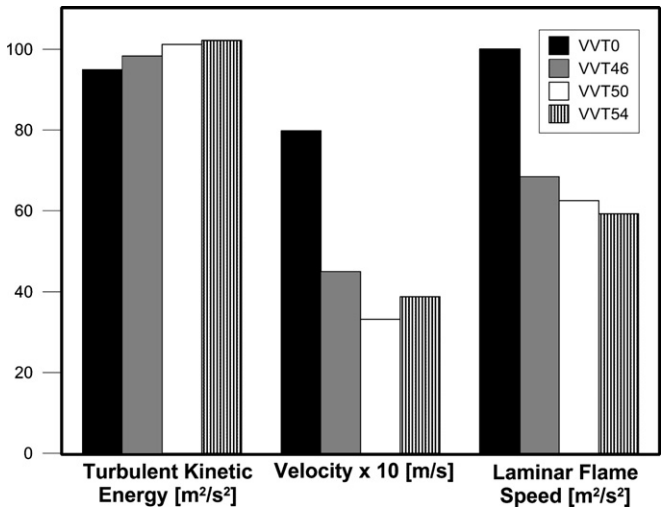

Fig. 22. Turbulent kinetic energy, actual flow velocity, laminar flame speed. Mean values calculated in a 5 mm radius sphere, centred at the spark-plug, at the spark time.

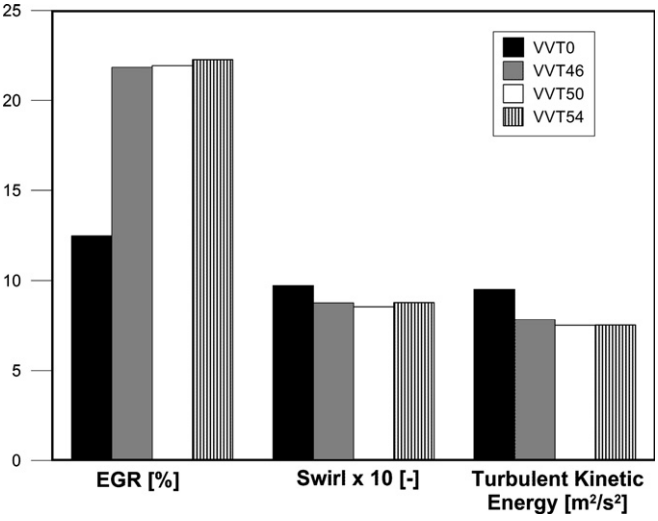

Fig. 21. Mean values in the combustion chamber for: residual gas fraction, swirl number and turbulent kinetic energy. Values calculated at the combustion top dead center.

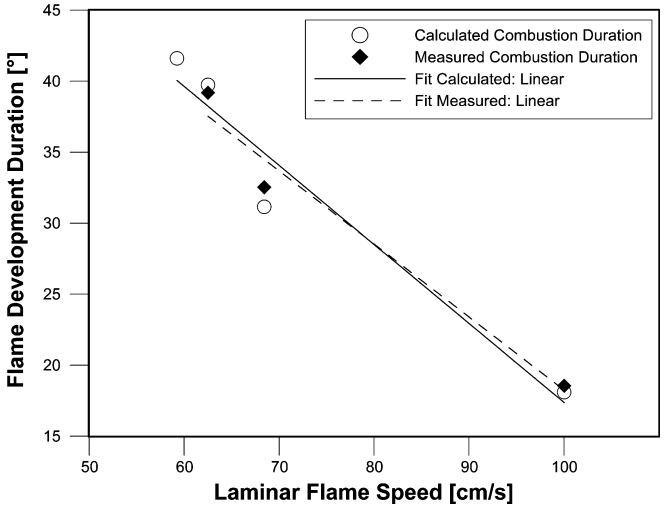

Fig. 23. Relationship between the laminar flame speed and the combustion duration of the flame development stage (0–5%).

The pressure rise is strongly influenced by the spark advance. Retarded valve timings (VVT46, VVT50, VVT54) show quite similar trends, while the standard VVT0 exhibits a faster pressure rise.

Thermodynamics and fluid-dynamics of the flow field within the cylinder can explain the trends of the flame front propagation rates.

As it is shown in Fig. 21, extremely retarded valve timings produce quite similar levels for swirl motion, turbulent kinetic energy and EGR as well. All this leads to quite similar flame propagation rates. On the contrary, the standard valve timing VVT0 performs a faster flame due to both a lower residual gas fraction and a higher turbulence level.

Dealing with the flame development stage, the air-fuel mixture conditions at the spark-plug zone and at the spark time have been investigated. In Fig. 22, the calculated values for the turbulent kinetic energy, the flow velocity and the laminar flame speed are reported.

It is easy to see that the laminar flame speed strongly influences the combustion duration of the 0-5% step. The relationship between these two variables is shown in Fig. 23. The flame development time decreases almost linearly as the laminar flame speed increases. The coefficient of determination of the linear fit is 0.94 with respect to the calculated data and 0.97 with respect to the calculated combustion durations.

4. Conclusions

The improvement in fuel economy, of a small spark-ignition engine, deriving from adopting a variable valve timing for load control has been evaluated by means of 1-D and 3-D numerical analyzes. The obtained results are in good agreement to the experimental data provided by engine manufacturer's research centre.

As it has been explained in the paper, the engine under study is characterized by a simple VVT technology mainly aimed to improve the engine efficiency at part load. Thus, the intake and exhaust processes have been optimized adopting such particular features as reverse Miller cycle, internal EGR and variable swirl generation.

The details of charge motion within the cylinder, the residual gas mass distribution and the intake and exhaust valve and port

capability in generating organized fluid motion have been analyzed at a given engine speed and several engine loads. The trend of calculated swirl numbers is worthy of note. A weak swirl motion is generated by the intake port at high valve lifts, while a major swirl level is produced by the exhaust backflow thorough the masked exhaust port at low lifts. This is an interesting result when the high EGR rates available at extremely retarded valve points have to be accounted for. The late valve close permits to reduce load with a significant de-throttle effect but, at the same time, generates large residual gas fractions. These could be favourable in both NO_x formation and load control, but they lower the combustion rate and the engine thermal efficiency while CO and HC formation could worsen. In engine operating points characterized by valve timing yielding high EGR rates, improvements in combustion quality through intense turbulence level of the charge could be effective. In this way, a meaningful contribution derives from the exhaust swirl generated by the re-aspired burnt gases through the masked exhaust port.

The VVT system here described, is resulted a useful system in optimizing both torque delivery and fuel consumption at part load operation. The variable cam phaser equipping a single camshaft is a cheap and reliable solution for varying the engine valve timing. Utilized in addition to proper choices for other engine parameters (see port, valve and combustion chamber design) it could be able to meet the target of improved fuel economy at a given performance and emission level.

References

[1] Stone R. Introduction to internal combustion engines. 3rd ed. Great Britain: Society of Automotive Engineers; 1999.

[2] Tuttle JH. Controlling engine load by means oflate intake-valve closing. In: SAE paper No. 800794 in the automotive engineering congress and exposition; 1980.

[3] Stein RA, Galietti KM, Leone TG. Dual equal VCT-A variable camshaft timing strategy for improved fuel economy and emissions. In: SAE technical paper series 950975; 1995.

[4] Fiorenza R, Pirelli M, Torella E, et al. Variable swirl and internal EGR by VVT application on small displacement 2 valve SI engines: an intelligent technology combination. In: FISITA 2004 world automotive congress. May 23–27.

[5] Fiorenza R, Pirelli M, Torella E, et al. VVT+port deactivation application on a small displacement SI 4 cylinder 16 valve engine: an effective way to reduce vehicle fuel consumption. In: SAE paper No. 2003-01-0020 in the SAE 2003 world congress; 2003.

[6] Tatschl R, Wieser K, Reitbauer R. Multidimensional simulation of flow evolution, mixture preparation and combustion in a 4-valve SI engine. In: Proceedings of the international symposium COMODIA 94; 1994. p. 139–49.

[7] Tatschl R et al. Rapid meshing and advanced physical modeling for gasoline DI engine application. In: International multidimensional modeling user's group meeting at the SAE congress; 2000.

[8] AVL FIRE Version 7 Handbook. Graz: AVL Internal Report; 2000.

[9] Spalding DB. Combustion and mass transfer. Oxford, UK: Pergamon Press; 1979.

[10] Cant RS, Bray KNC. Strained laminar flamelet calculation of premixed turbulent combustion in a closed vessel. In: Proceedings of 22nd international symposium on combustion; 1990. p. 809–15.

[11] El Tahry SH. A turbulent-combustion model for homogeneous charge engines. Combust Flame 1990;79:122–40.

[12] Choi CR, Huh KY. Development of a coherent flamelet model for a spark-ignited turbulent premixed flame in a closed vessel. Combust Flame 1998;114:336–48.

[13] Meneveau C, Poinsot T. Stretching and quenching of flamelets in premixed turbulent combustion. Combust Flame 1991;86:311–32.

[14] Blint RJ. The relationship of the laminar flame width to flame speed. Combust Sci Technol 1986;49:79–92.

[15] Metghalchi M, Keck JC. Burning velocities of mixtures of air with methanol, isooctane and indolene at high pressure and temperature. Combust Flame 1982;48:191–210.

[16] Heywood JB. Internal combustion engines. New York, NY: McGraw-Hill Publishing Co.; 1998.

[17] Rutland CJ, Pieper CM, Hessel R. Intake and cylinder flow modeling with a dual-valve port. In: SAE Paper No. 930069 in the SAE international congress and exposition; 1993.

[18] Caufield S, Rubenstein B, Martin JK, et al. A comparison between CFD predictions and measurements at inlet port discharge coefficient and flow characteristics. In: SAE Paper No. 1999-01-3339 in the small engine technology conference and exposition; 1999.

[19] Bianchi GM, Cantore G, Fontanesi S. Turbulence modeling in CFD simulation of ICE intake slows: the discharge coefficient prediction. In: SAE Paper No. 2002-01-1118 in the SAE 2002 world congress; 2002.

[20] Hires SD, Tabaczynski RJ, Novak JM. The prediction of ignition delay and combustion intervals for a homogeneous charge spark ignition engine. In: SAE Trans., vol. 87, Paper No. 780232; 1978.

[21] Fontana G, Galloni E, Palmaccio R. Development of a new intake system for a small spark-ignition engine: modeling the flow through the inlet valve. In: SAE Paper No. 2003-01-0369 in the SAE 2003 world congress; 2003.

[22] Wu C, Puzinauskas PV, Tsai JS. Performances analysis and optimization of a supercharged Miller cycle Otto engine. Appl Therm Eng 2003;23:511–21.

[23] Hara S, Nakajima Y, Nagumo S. Effects of intake valve closing timing on SI engine combustion. In: SAE Technical Paper Series 850074; 1985.

[24] Fontana G, Galloni E, Torella E. Experimental and numerical analysis of a small VVT S.I. engine. In: SAE Paper No. 2005-24-079 in the 7° international conference on engines for automobile ICE2005; 2005.

[25] Fontana G, Galloni E, Palmaccio R, Torella E. The influence of variable valve timing on the combustion process of a small spark-ignition engine. In: SAE Paper No. 2006-01-0445 in the SAE 2006 world congress; 2006.